environmental microbiology

Environmental Microbiology (2018) **20**(12), 4297–4313 doi:10.1111/1462-2920.14343

Metabolic potential of microbial communities from ferruginous sediments

Aurèle Vuillemin,[1,2*] Fabian Horn,[1] André Friese,[1] Matthias Winkel,[1] Mashal Alawi,[1] Dirk Wagner,[1,3] Cynthia Henny,[4] William D. Orsi,[2,5] Sean A. Crowe[6,7] and Jens Kallmeyer[1]

[1]*GFZ German Research Centre for Geosciences, Helmholtz Centre Potsdam, Section 5.3: Geomicrobiology, Potsdam, Germany.*

[2]*Department of Earth & Environmental Sciences, Paleontology & Geobiology, Ludwig-Maximilians-Universität München, Munich, Germany.*

[3]*University of Potsdam, Faculty of Mathematics and Natural Sciences, Institute of Earth and Environmental Sciences, Potsdam, Germany.*

[4]*Research Center for Limnology (LIPI), Indonesian Institute of Sciences, Division of Inland Waterways Dynamics, Cibinong-Bogor, Indonesia.*

[5]*Geobio-CenterLMU, Ludwig-Maximilians-Universität München, Munich, Germany.*

[6]*Department of Microbiology and Immunology, University of British Columbia, Vancouver, Canada.*

[7]*Department of Earth, Ocean and Atmospheric Sciences, University of British Columbia, Vancouver, Canada.*

Summary

Ferruginous (Fe-rich, SO_4-poor) conditions are generally restricted to freshwater sediments on Earth today, but were likely widespread during the Archean and Proterozoic Eons. Lake Towuti, Indonesia, is a large ferruginous lake that likely hosts geochemical processes analogous to those that operated in the ferruginous Archean ocean. The metabolic potential of microbial communities and related biogeochemical cycling under such conditions remain largely unknown. We combined geochemical measurements (pore water chemistry, sulfate reduction rates) with metagenomics to link metabolic potential with geochemical processes in the upper 50 cm of sediment. Microbial diversity and quantities of genes for dissimilatory sulfate reduction (*dsrAB*) and methanogenesis (*mcrA*) decrease with increasing depth, as do rates of potential sulfate reduction. The presence of taxa affiliated with known iron- and sulfate-reducers implies potential use of ferric iron and sulfate as electron acceptors. Pore-water concentrations of acetate imply active production through fermentation. Fermentation likely provides substrates for respiration with iron and sulfate as electron donors and for methanogens that were detected throughout the core. The presence of ANME-1 16S and *mcrA* genes suggests potential for anaerobic methane oxidation. Overall our data suggest that microbial community metabolism in anoxic ferruginous sediments support coupled Fe, S and C biogeochemical cycling.

Introduction

Ferruginous conditions are rich in iron and poor in sulfate, and were widespread in the Archean and Proterozoic oceans (Poulton and Canfield, 2011). However, the diversity and metabolic potential of microbial communities living in anoxic ferruginous sediments remain poorly known. The Malili Lake System of Indonesia (Fig. 1A), which comprises five interconnected lakes (Matano, Towuti, Mahalona, Lontoa, Masapi) hosted in ophiolitic and (ultra) mafic rocks (Haffner *et al.,* 2001; Crowe *et al.,* 2008a), likely hosts biogeochemical processes analogous to those that could have operated in the Archean ferruginous ocean. The tropical climate and lateritic weathering of the catchment cause a strong flux of iron (oxy)hydroxides to these lakes but little sulfate. These detrital inputs, which mostly consist of goethite (α-FeOOH) and ferrihydrite ($Fe_2O_3 \cdot 0.5H_2O$) along with some hematite (Fe_2O_3) and magnetite (Fe_3O_4) (Crowe *et al.,* 2004), lead to ferruginous (iron-rich) conditions with phosphorus scavenging by iron oxides in the water column (Crowe *et al.,* 2008a; Zegeye *et al.,* 2012). As a result, Lake Matano and by extension Lake Towuti is among the least productive tropical lakes on Earth (Crowe *et al.,* 2008b). Under permanent stratification and persistent anoxia, as for instance in the deep basin of Lake Matano, a substantial part of the organic matter (OM) is remineralized through methanogenesis (Crowe *et al.,* 2011).

Received 27 February, 2018; revised 22 May, 2018; accepted 25 June, 2018. *For correspondence. E-mail a.vuillemin@lrz.uni-muenchen.de; Tel. +49 (0)89 2180-6659; Fax +49 (0)89 2180-6601

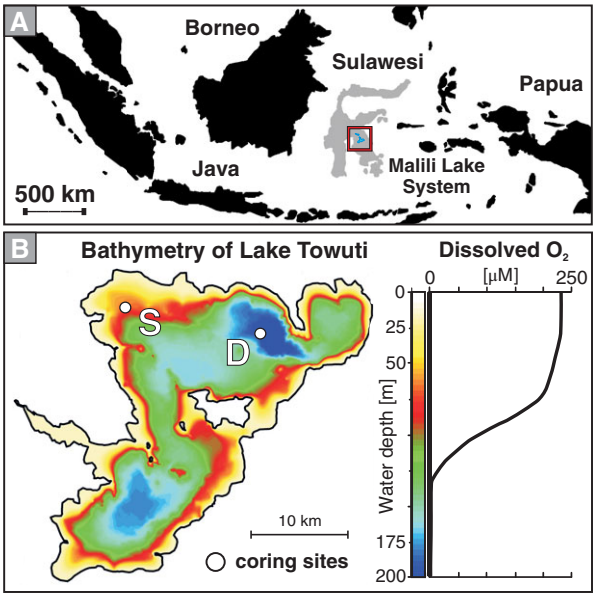

Fig. 1. Lake Towuti location, drilling site map and water body conditions.
A. Map of Indonesia displaying the location of Sulawesi Island and the Malili Lake System.
B. Bathymetric map of Lake Towuti (modified after Russell *et al.,* 2016) displaying the shallow (S: 60 m water depth) and deep (D: 200 m water depth) sites at which gravity cores were retrieved, and oxygen profile measured in the water column, with an oxycline occurring in between 90 and 130 m depth.

Unlike upstream Lake Matano, which is permanently stratified and anoxic below 110 m water depth (Katsev *et al.,* 2010), Lake Towuti (2.5°S, 121°E), has been inferred to mix at least occasionally (Costa *et al.,* 2015). Sporadic mixing could affect the distribution of phosphate in the water column (Katsev *et al.,* 2010) and potentially influence its productivity (Bramburger *et al.,* 2008; Russell *et al.,* 2016). Lake Towuti has a maximum water depth of ca. 200 m, is presently oxygen-depleted below 130 m depth (Fig. 1B) with a circumneutral (pH ~7.8), weakly conductive (210 μS cm^{-1}) and weakly thermally stratified (i.e. 31–28°C) water column (Haffner *et al.,* 2001; Vuillemin *et al.,* 2016). Because freshwater ecosystems often display a depletion of sulfate and enrichment of ferrous iron in pore water at shallow depths, microbial communities evolving under ferruginous geochemical conditions could be more widespread than previously thought (Norði *et al.,* 2013; Bravo *et al.,* 2018). Recent geomicrobiological investigations of Lake Towuti sediments showed that despite extremely low sulfate concentrations (<20 μM), biogeochemical processes related to sulfur, iron and methane transformations can co-occur in the sediment (Vuillemin *et al.,* 2016). This led to the hypothesis that cryptic sulfur cycling could be supported through sulfide re-oxidation with ferric iron. Cryptic sulfur cycling has been extensively studied in the marine (Canfield *et al.,* 2010; Holmkvist *et al.,* 2011) and lacustrine realm (Norði *et al.,* 2013; Hansel *et al.,* 2015) from both geochemical (Thamdrup *et al.,* 1994; Zopfi *et al.,* 2004) and microbiological perspectives (Thamdrup *et al.,* 1993; Milucka *et al.,* 2012). However, the composition and structure of microbial communities that contribute to cryptic sulfur cycling remain largely unknown (Meyer and Kuever, 2007; Stewart, 2011; Aoki *et al.,* 2015). In addition, anaerobic oxidation of methane (AOM) is often reported as a potential sink in ferruginous settings, raising the possibility that alternative electron acceptors like Fe^{3+} may play a role (Beal *et al.,* 2009; Crowe *et al.,* 2011; Sivan *et al.,* 2011; Norði *et al.,* 2013; Ettwig *et al.,* 2016).

Here, we leverage previous biogeochemical analyses of Lake Towuti surface sediment (Vuillemin *et al.,* 2016, 2017) to frame metabolic potential recovered from intracellular DNA (iDNA) extracted from short (< 50 cm) sediment cores retrieved from two different sites in Lake Towuti (Fig. 1B). We quantified potential sulfate reduction rates (pSRR) via radiotracer incubations and determined concentrations of various reduced inorganic sulfur compounds to explore sulfur cycling and its possible connection to iron cycling through re-oxidation of reduced sulfur compounds. We reconstruct microbial diversity using 16S rRNA gene distributions and abundances and examine metabolic potential of microbial communities using functional marker genes. We evaluate the distribution of microorganisms taxonomically affiliated with known sulfate-reducing (SRB) and iron-reducing bacteria (FeRB) as well as those related to known methanogens and syntrophs involved in hydrogen production and transfer.

Results

Pore water chemistry, sulfate reduction rate, Total reduced inorganic sulfur

As expected in ferruginous environments, pore water SO_4^{2-} concentrations (Fig. 2) were mainly in the single μM range and often close to the quantification (8.4 μM) and detection (2 μM) limits and H_2S was always below our detection limit (1 μM). At the shallow site, SO_4^{2-} concentrations were higher, with values around 20 μM in the uppermost 4 cm below lake floor (cmblf), decreasing gradually to our detection limit at the base of the core. At the deep site, all SO_4^{2-} concentrations were close to our detection limit. Dissolved Fe^{2+} concentrations at the shallow site fluctuated between 0 and 10 μM with a slight increase below 10 cmblf, whereas at the deep site Fe^{2+} increased from 40 to 50 μM with depth with a slight excursion to lower values (30 μM) in the upper 6 cmblf. Formate concentrations at the shallow site (Fig. 2) decreased with depth from 40 to 10 μM within the upper 5 cmblf before increasing again to 20 μM. Acetate

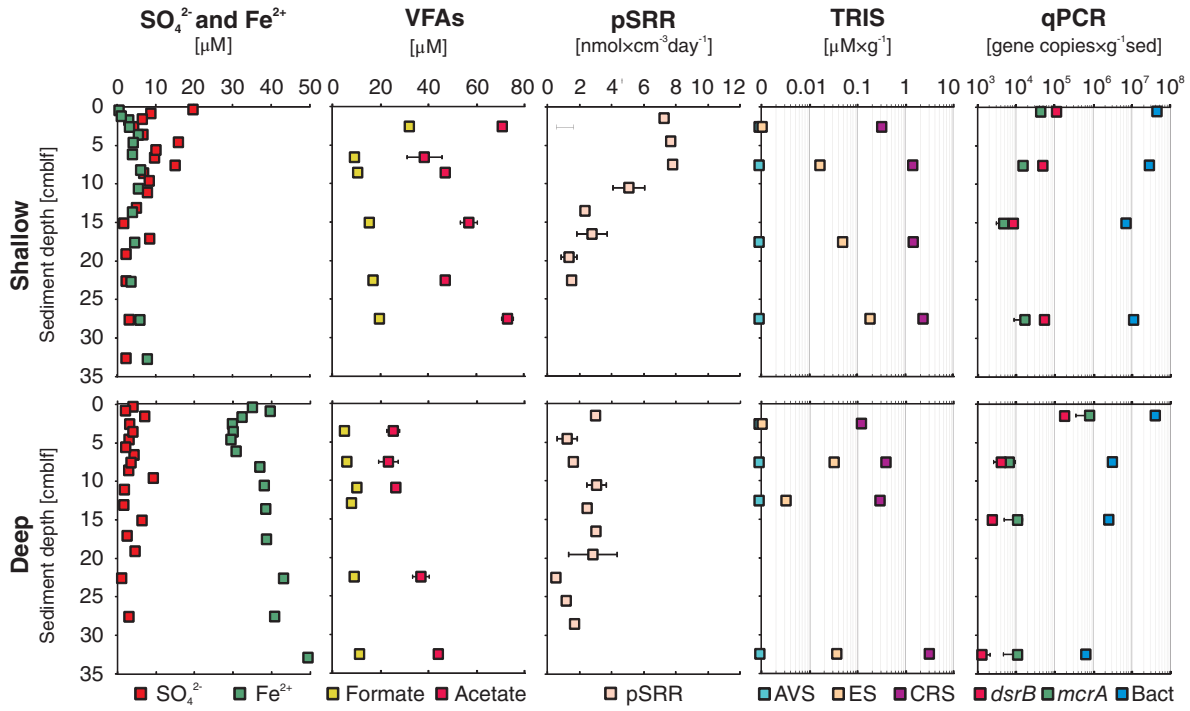

Fig. 2. Multiple profiles established on short sediment cores. From left to right: Sulfate and dissolved ferrous iron concentrations [μM] measured in the pore water; formate and acetate concentrations [μM] measured in pore water; pSRR [nmol × cm^{-3} day^{-1}] obtained after 24 h incubation experiments; TRIS compounds [μmol × g^{-1}] in log scale measured in sediments as AVS or monosulfides, ES and CRS or disulfides; gene copies per g^{-1} wet sediment based on qPCR assays with primer pairs targeting the bacterial 16S rRNA, *dsrB* and *mcrA* gene.

concentrations also decreased in the upper 5 cmblf from 70 to 40 μM and, in spite of some scatter, increased again with depth to 70 μM. At the deep site, formate concentrations were all close to quantification and detection limits, with values increasing from 5 to 11 μM with depth. Similarly, acetate concentrations displayed values increasing from 25 to 45 μM with depth.

Potential SRR differed in rates and depth distribution (Fig. 2) between the two sites. The shallow site displayed maximum rates (7 nmol cm^{-3} day^{-1}) within the upper 10 cmblf. Below this depth, rates decreased sharply to 2 nmol cm^{-3} day^{-1}. At the deep site, rates were much lower (1 to max. 3 nmol cm^{-3} day^{-1}) and did not show any depth trend. Because SO_4^{2-} concentrations were often well below the lower limit of quantification (8.4 μM), the absolute values of the pSRR have to be taken with caution. Distribution of the different fractions comprising the total reduced inorganic sulfur (TRIS) in the sediment was analysed by sequential extraction. Three fractions were separated: (1) acid volatile sulfur (AVS), consisting mainly of monosulfides and free hydrogen sulfide, (2) chromium reducible sulfide (CRS), consisting mainly of more crystalline disulfides like pyrite (i.e. FeS_2), and (3) elemental sulfur (ES). At both sites CRS was the largest TRIS fraction, although minimal amounts of ES were detected in all but the uppermost samples at both sites (Fig. 2). At the shallow site, CRS values increased gradually with depth from 0 to 2.5 μmol × g^{-1}, whereas at the deep site values were close to 0.1 in the upper half of the core and highest in the lowermost sample, reaching 3 μmol × g^{-1}. AVS was below detection at both sites.

Quantitative PCR

At the shallow site, the quantity of 16S rRNA, *dsrB*, and *mcrA* gene copies decreased gradually from the surface down to 15 cmblf, then slightly increasing again towards the bottom of the core. At the deep site, values showed a steep drop in the upper 7 cmblf and remained more or less stable throughout the rest of the core (Fig. 2). At the shallow site, bacterial 16S rRNA genes in the uppermost sediment corresponded to 4.43 × 10^7 gene copies × g^{-1} (wet sediment) decreasing to 1.11 × 10^7 at the bottom of the core. Similarly, *dsrB* genes decreased from 1.09 × 10^5 to 5.31 × 10^4 gene copies × g^{-1}, while *mcrA* genes displayed overall lower copy numbers decreasing from 4.24 × 10^4 to 1.66 × 10^4 gene copies ×g^{-1} with depth. In comparison to the shallower site, bacterial 16S rRNA genes at the deep site showed lower copy numbers in the uppermost sample (4.11 × 10^7 gene copies × g^{-1}), decreasing to 6.64 × 10^5 gene copies × g^{-1} at the bottom of the core. Contrary to the shallow site,

dsrB genes showed higher copy numbers than *mcrA* genes at all depth of the deep site, gradually decreasing from 1.72×10^5 gene copies $\times$ g^{-1} in surface sediment to 1.25×10^3 gene copies $\times$ g^{-1} at the bottom of the core. *McrA* genes gradually decreased from 7.63×10^5 to 1.05×10^4 gene copies $\times$ g^{-1} with depth. The quantity of *mcrA* and *dsrB* genes were generally two to three orders of magnitude lower than 16S rRNA gene copies at all sites and depths.

Diversity of 16S rRNA genes

The sum of 16S rRNA gene OTUs affiliated with SRB groups decreased with sediment depth from about 35 to less than 10% of total reads. Their relative abundance dropped between 1 and 7 cmblf (Fig. 3). Because the deltaproteobacterial Candidate Sva0485 clade is commonly found in active sulfate-reducing assemblages and is assumed capable of sulfate reduction (Concheri *et al.,* 2017), it is listed among taxa affiliated with known SRB. Representative sequences corresponding to SRB (Fig. 4) were mainly affiliated with *Thermodesulfovibrio* and *Desulfuromonas. Desulfobacca, Desulfurosporosinus,* and *Desulfurispora* were also identified, with the addition of some other minor OTUs (e.g. *Desulforegula*, *Desulfobulbus*, *Desulfatiglans*, *Desulfarculus*).

Relative abundances of taxa affiliated with FeRB fluctuated between 8% and 15% of total reads but overall increased with depth at both sites (Fig. 3). Bacteriovoracaceae represented ca. 5% of all reads, but decreased to 1% with depth at the deep site, whereas Geobacteraceae became gradually more abundant with depth, representing approximately 10% of all reads in lowermost sediments of the deep site. Only few Firmicutes and Acidobacteria were affiliated with groups known to perform iron reduction including members of the Peptococcaceae (Zavarzina *et al.,* 2007) and Holophagaceae (Nevin and Lovley, 2002). The taxonomic affiliations of the corresponding OTUs were *Deferrisoma*, *Geobacter*, *Thermincola* and *Geothrix* clades (Fig. 4).

At the shallow site, the relative abundance of OTUs affiliated with known syntrophic bacteria (Sieber *et al.,* 2012) were minor in uppermost and lowermost sediment layers and included Syntrophaceae, Syntrophomonadaceae and Peptococcaceae (Fig. 3). Potential syntrophs were also affiliated with Ruminococcaceae and Clostridiales Family XVIII (Thauer *et al.,* 2008), which were only present in the lowermost samples of the deep site where they accounted for up to 12% of all reads (Fig. 3). The taxonomic affiliations of their representative OTUs were Clostridiales, Ruminococcaceae, *Smithella*, *Pelotomaculum*, *Pelospora*, *Syntrophothermus* and some uncultured Syntrophaceae (Fig. 4).

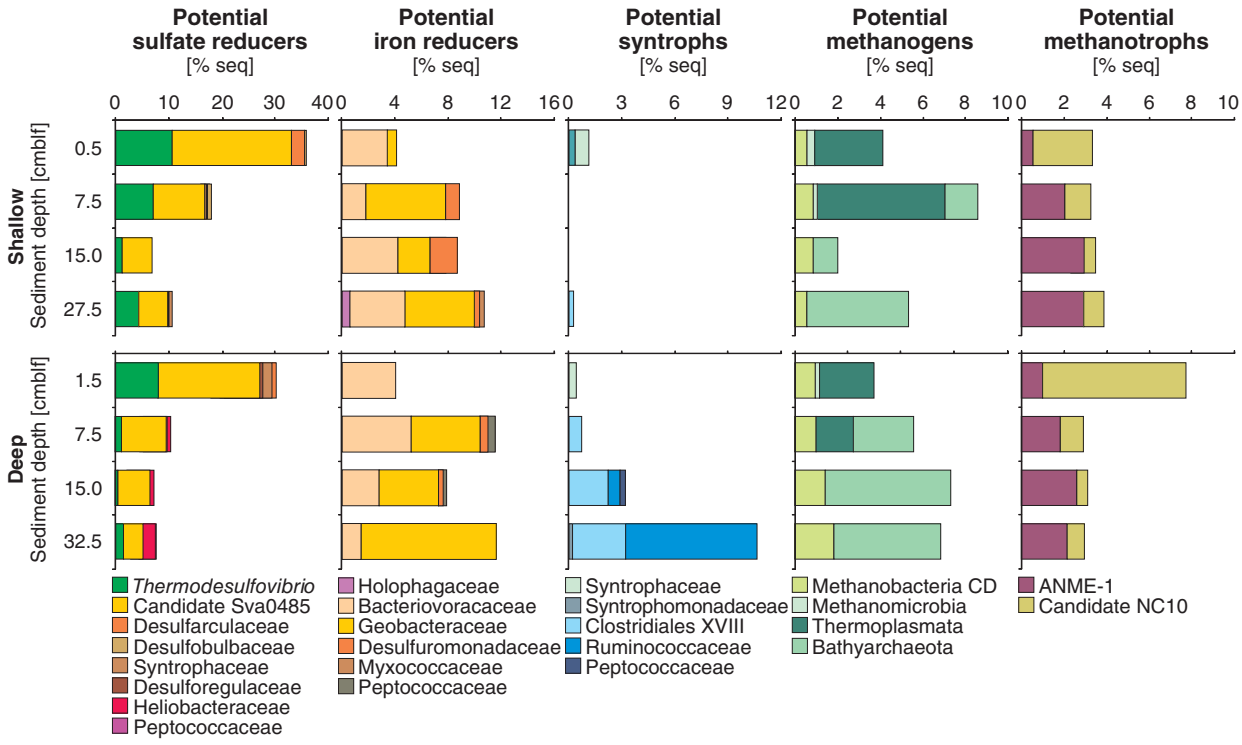

Fig. 3. Relative abundances of OTUs related to taxa with proven phenotypes in sulfur, iron and hydrogen cycling. From left to right: Bar charts displaying relative abundances [% seq] of taxa closely affiliated (> 97%) with known sulfate-reducing bacteria, FeRB, hydrogen syntrophs, methanogens and anaerobic methanotrophs.

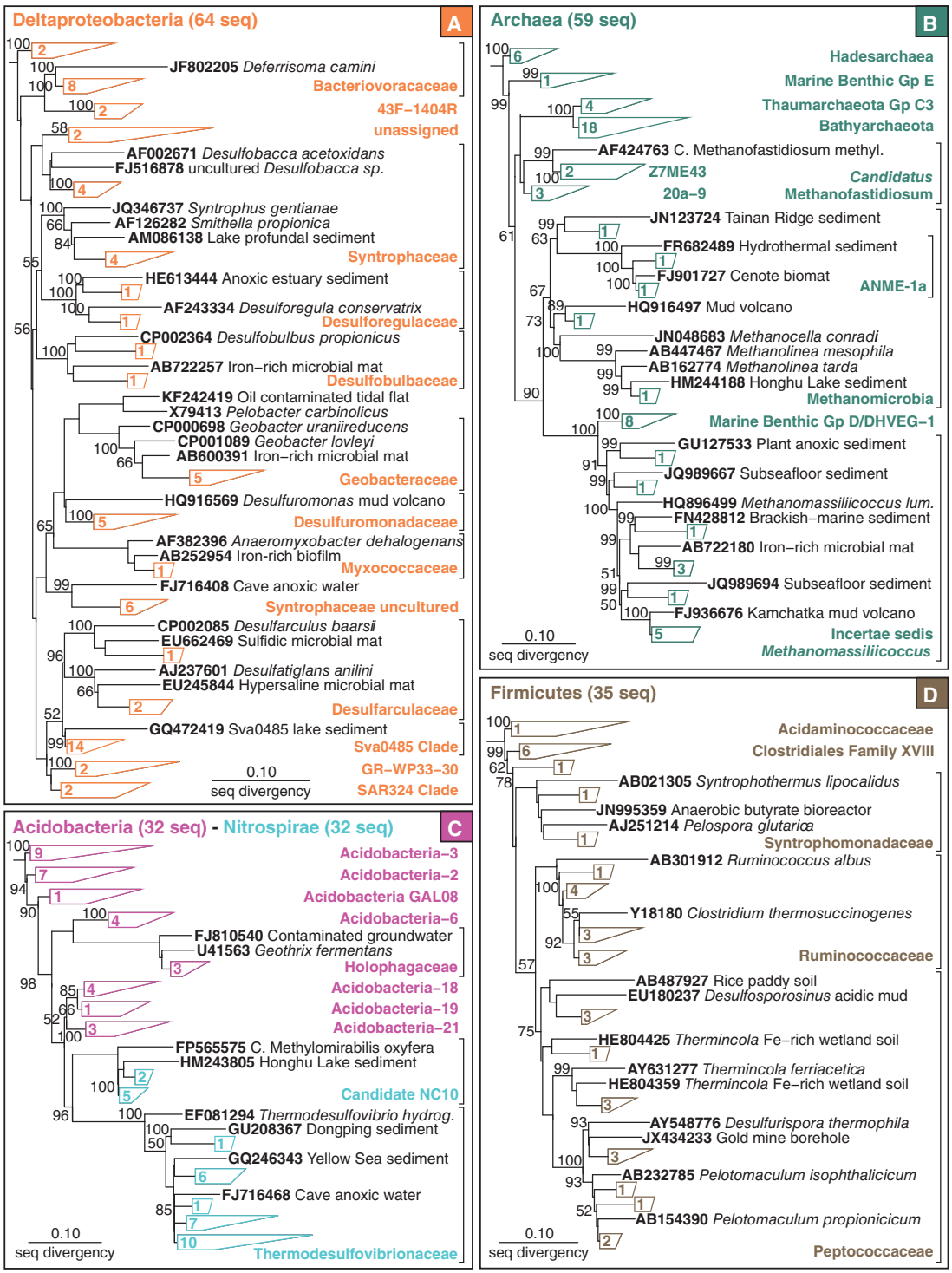

Fig. 4. Phylogenetic trees based on partial 16S rRNA gene sequences established for representative OTUs related to sulfur, iron, and methane cycling.
A. Deltaproteobacteria.
B. Archaea.
C. Acidobacteria and Nitrospirae.
D. Firmicutes. Sequences identified as potential SRB are mostly affiliated with *Desulfobacca, Thermodesulfovibrio, Desulfurispora* and *Desulfosporosinus.* Those related to potential FeRB are represented by *Deferrisoma*, *Geobacter*, *Geothrix*, and *Thermincola.* Sequences of potential syntrophs include *Smithella*, *Pelotomaculum*, *Syntrophothermus*, *Pelospora*, along with candidates among Clostridiales and Ruminococcaceae. Methanogen-related sequences are *Methanolinea*, *Methanomassiliicoccus*, *Candidatus* Methanofastidiosum and Bathyarchaeota. Sequences of anaerobic methanotrophs are represented by the ANME-1a group.

At both sites, relative abundances of OTUs assigned to methanogens accounted for ca. 4% to 9% of all reads (Fig. 3). Below 7.5 cmblf at the shallow site, values dropped to 3% and then increased again to 6%. At the deep site, relative abundances increased gradually with depth from 4% to 8%. OTUs of this fraction mainly corresponded to Thermoplasmata, Methanomicrobia, Methanobacteria, as well as Bathyarchaeota, although the capacity of Bathyarchaeota to conduct methanogenesis remains unsubstantiated through direct measurements of metabolism. Although, the overall relative abundance of bathyarchaeotal OTUs increased with depth from ca. 10% to 50% at both sites (Supporting Information), we listed only those related to population genomes with inferred metabolic potential for methanogenesis (Evans *et al.,* 2015), which summed up to 5% of all reads. Taxonomic assignments of representative sequences related mainly to the Incertae Sedis *Methanomassiliicoccus* cluster (Fig. 4). Multiple OTUs were identified as *Candidatus* Methanofastidiosum, *Methanolinea* being also present with one single OTU. Among the 136 taxa related to Bathyarchaeota (Supporting Information), 18 OTUs had a close phylogenetic affiliation to population genomes with inferred metabolic potential for methanogenesis (Evans *et al.,* 2015).

OTUs listed as potential anaerobic methanotrophs were affiliated with Candidate NC10 (He *et al.,* 2015) and ANME-1 (Boetius *et al.,* 2000; Meyerdierks *et al.,* 2010). Their relative abundance remained constant with depth at ca. 4% of all reads, except in the uppermost part of the deep site with 7% of NC10 reads (Fig. 3). However, methane oxidation via NO-dismutation was only demonstrated for *Candidatus* Methylomirabilis*,* the only cultivated member of the candidate phylum NC10 (He *et al.,* 2015). Taxonomic assignments confirmed the presence of both *Candidatus* Methylomirabilis and ANME-1 in the consortia (Fig. 4).

The canonical correspondence analysis (CCA) (Supporting Information) showed that at both sites the differences in communities can be explained by depth or by other factors that also change with depth (e.g. cell counts, SO_4^{2-} and Fe^{2+}concentrations, pSRR). Relative abundances and numbers of representative OTUs are summarized in Supporting Information Table S1.

Taxonomic affiliations of functional genes

Within the metagenomes, we detected open reading frames (ORFs) that encode proteins homologous to the formate-tetrahydrofolate ligase (*fhs*), formate dehydrogenase (*fdh*), dissimilatory sulfite reductase subunit alpha and beta (*dsrAB*), adenylylsulfate reductase subunit alpha and beta (*aprAB*), anaerobic sulfite reductase subunit alpha (*asrA*), thiosulfate/polysulfide reductase subunit alpha (*phsA*), sulfhydrogenase subunit beta (*hydB*), methyl-coenzyme M reductase subunit alpha to gamma (*mcrA*), methanol coenzyme M methyltransferase subunit beta (*MtaB*), methylamine-specific coenzyme M methyltransferase subunit alpha (*MtbA*), methylthiol coenzyme M methytransferase subunit alpha (*mtsA*), carbon-monoxide dehydrogenase (*CODH*), acetyl-CoA decarbonylase subunit alpha (*cdhA*), and tetrahydromethanopterin S-methyltransferase alpha subunit (*mtrA*). These ORFs were most similar to groups that were also present in the 16S rRNA gene datasets (e.g. Bathyarchaeota, Deltaproteobacteria), indicating the functional potential for utilization of a wide range of sulfur and carbon substrates (Fig. 5).

For example, the *fhs* and *fdh* genes (Fig. 5A, left) were largely affiliated with taxa within the Deltaproteobacteria, Firmicutes and Chloroflexi with about 30% of other sequences affiliating with the Omnitrophica, Aminicenantes, Bathyarchaeota and Atribacteria (Supporting Information), indicating production and consumption of formate and acetate by non-methanogenic taxa. Most *dsrAB* predicted protein sequences derived from sulfate reducing Deltaproteobacteria, Firmicutes and Nitrospirae, although other *dsrAB* predicted proteins also had an affiliation to the Chloroflexi and a number of bacterial candidate phyla. Interestingly, many of the *dsrAB* genes were recovered from various uncultivated Deltaproteobacteria (Fig. 5A), which could include the Sva0485 clade presently listed as potential SRB in the 16S rRNA gene dataset (Fig. 3). Consistent with this result, most of the *aprAB* genes were also affiliated with the Deltaproteobacteria, Firmicutes and Nitrospirae. The same applies to the *asrA* and *phsA* genes, indicating that sulfite and thiosulfate could be used as electron acceptors by Deltaproteobacteria, Firmicutes and Chloroflexi. Taxonomic assignment of the *hydB* genes, which are indicative of the metabolic potential to reduce polysulfide, revealed a majority of Bathyarchaeota, with nevertheless some Chloroflexi and Deltaproteobacteria.

Sequences of the *mcrA* gene were mostly affiliated with the ANME-1 group, Methanobacteria, Methanomicrobia and the Bathyarchaeota (Fig. 5A, right). Sequences of the *MtaB* gene indicated that Methanomicrobia, Hadesarchaea and Firmicutes have the metabolic potential to use methanol. Although scarce, *MtbA* and *mtsA* gene sequences indicated that some members among the Bathyarchaeota, Methanomicrobia, and Hadesarchaea clades could use methylamines and methylated thiols as carbon substrates. Detection of *CODH* gene was affiliated with the Bathyarchaeota, Hadesarchaea, Deltaproteobacteria, Firmicutes and Chloroflexi. It presently indicates the metabolic potential of these clades to use carbon monoxide as an electron acceptor anaerobically, even though this gene is also found in aerobic bacteria. Similarly, sequences of the *cdhA* gene were most abundant and related mainly to Bathyarchaeota and Methanomicrobia, likely showing that methanogens are mainly autotrophs (Sarmiento *et al.,* 2013; Lang *et al.,* 2015). Affiliations of the *mtrA* genes showed that the

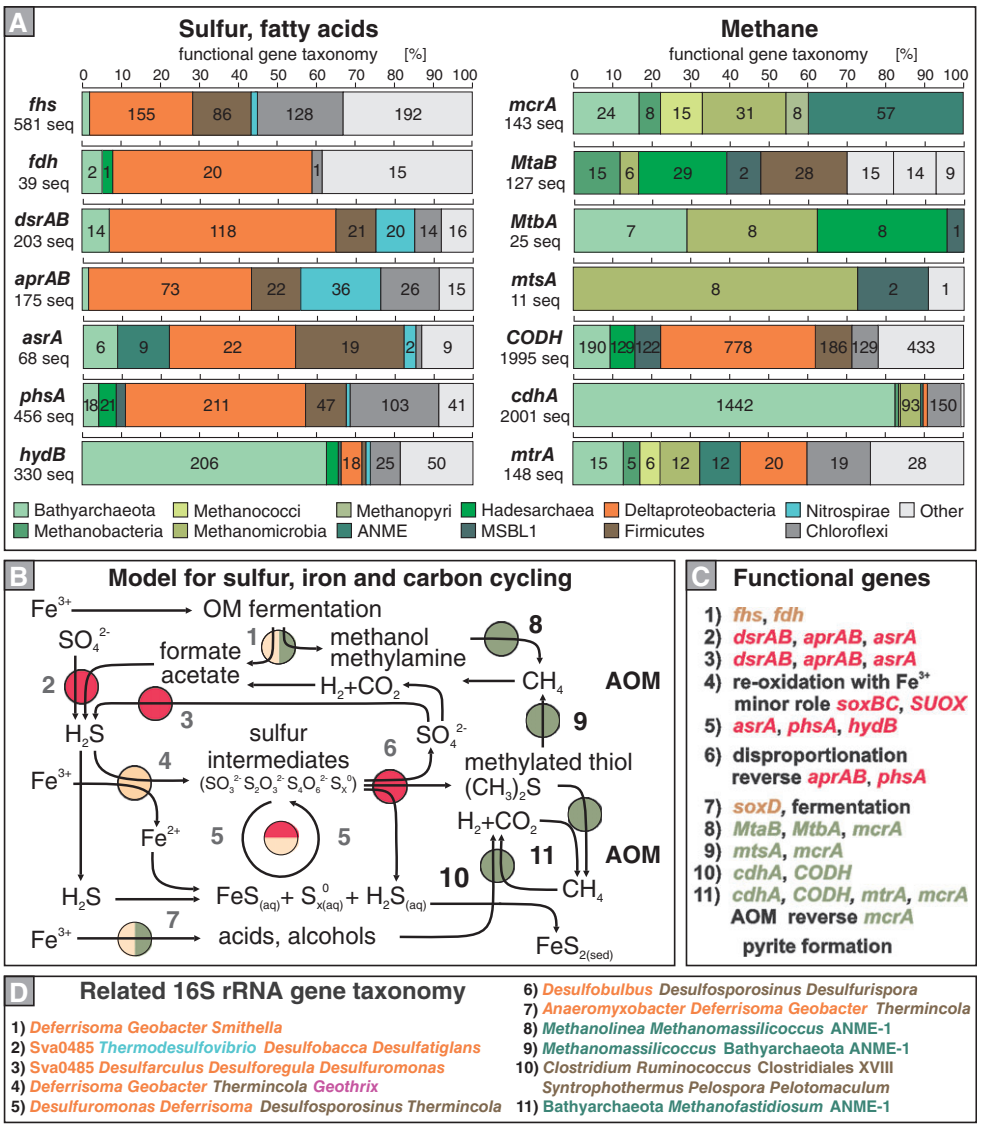

Fig. 5. Affiliations of functional genes, reactions involved in sulfur, iron and methane cycling, with functional genes and 16S rRNA gene taxonomy related to the reactions.
A. Taxonomic assignment for subunits of functional genes corresponding to: (right) formate-tetrahydrofolate ligase (*fhs*), formate dehydrogenase (*fdh*), dissimilatory sulfite reductase (*dsrAB*), adenylylsulfate reductase (*aprAB*), anaerobic sulfite reductase (*asrA*), thiosulfate/polysulfide reductase (*phsA*), sulfhydrogenase or sulfur reductase (*hydB*); (left) methyl-coenzyme M reductase (*mcrA*), methanol coenzyme M methyltransferase (*MtaB*), methylamine-specific coenzyme M methyltransferase (*MtbA*), methylthiol coenzyme M methytransferase (*mtsA*), carbon-monoxide dehydrogenase (*CODH*), acetyl-CoA decarbonylase (*cdhA*), and tetrahydromethanopterin S-methyltransferase (*mtrA*).
B. Sketch depicting the expected coupling of iron, sulfur and methane cycles (modified after Holmkvist *et al.,* 2011). Reactions related to iron (light brown circles) and sulfur (red circles) are listed from 1 to 7, whereas methylated compounds and hydrogen conversion to methane (green circles) is listed from 8 to 11.
C. List of functional genes respectively involved in sulfur (red) and methane (green) reactions.
D. Identified 16S rRNA gene taxa with predicted metabolic capabilities to drive iron, sulfur (1 to 7) and methane cycling (8 to 11).

metabolic capacity to use CO_2, and acetate, was present in Bathyarchaeota, Methanobacteria, Methanococci, Methanomicrobia, Deltaproteobacteria and Chloroflexi.

The relative abundance of ORFs homologous to sulfur-oxidation (*sox*) and sulfite oxidase (*SUOX*) genes, which are involved in the aerobic oxidation of sulfur compounds, was minimal (Supporting Information, Fig. S6). Most of these ORFs were derived from Cyanobacteria, Chlorobi and Betaproteobacteria, suggesting these were sourced from water column communities (Supporting Information).

Discussion

Interactions between sulfate and iron reduction

Measurements of pSRR revealed the potential sulfate reduction at both sites, although the rates were higher at

the shallow site (Fig. 2). Decreasing pSRR at the shallow site was correlated with a decline in relative abundances of 16S rRNA sequences affiliated with known SRB (Fig. 3) and clear changes in microbial community composition (Fig. 4). Because the 16S rRNA gene sequence is highly conserved and thus evolves slowly, a recovered environmental 16S rRNA gene sequence that is closely related (> 97%) to that of a cultivated strain, with a proven major biochemical phenotype, can be used loosely to infer a similar metabolic potential (Langille *et al.,* 2013). Our carefully curated phylogenetic analysis (Fig. 4) shows that many sequences recovered from these sediments have nearly identical 16S rRNA gene sequences to microorganisms with physiological capacity for sulfate and iron reduction, and methanogenesis. As microorganisms with this level of 16S rRNA gene sequence similarity can be different at the genome level (Louca *et al.,* 2016), we proceed cautiously in comparing OTUs to organisms with known metabolic phenotypes (e.g. iron reduction, sulfate reduction, methanogenesis). Where possible, we try to support predicted functions through comparisons to the taxonomic affiliation of a functional marker recovered from our metagenomes (Figs 3–5). We recognize, however, that horizontal gene transfer can lead to differences between the taxonomic affiliation of a functional marker and the taxonomy of the host organism.

Depths with the highest pSRR also had high relative abundances of *Thermodesulfovibrio* and *Desulfobacca.* In the laboratory, these genera grow through sulfate reduction mainly with formate, pyruvate and lactate as electron donors for the former (Sekiguchi *et al.,* 2008) and only acetate for the latter (Oude Elferink *et al.,* 1999). At the shallow site, transition to low pSRR (ca. 10 cmblf) correlated with the appearance of *Desulfuromonas*, a genus with cultured strains capable of reducing sulfate but also sulfur and iron (Greene, 2014; Pjevac *et al.,* 2014). In sediments of the deep site that exhibited lowest pSRR (Fig. 2), *Desulfuromonadales* were also present. Additionally, we identified taxa belonging to Firmicutes related to *Desulfurispora* (Kaksonen *et al.,* 2007) and *Desulfosporosinus* (Ramamoorthy *et al.,* 2006), which are known to reduce sulfate, sulfite, thiosulfate, ES and iron. We also found taxa affiliated with *Desulfobulbus*, which are related to organisms that in cultures can reduce sulfur and also produce SO_4^{2-} from ES in the presence of Fe^{3+}oxides (Castro *et al.,* 2000). Taxonomic affiliation of the *dsrAB* and *aprAB* genes provided additional information on the distribution of metabolic potential for sulfate reduction, which in Lake Towuti sediments includes members of the Deltaproteobacteria (e.g. *Desulfobacca*), Firmicutes (e.g. *Desulfosporosinus*) and Nitrospirae (e.g. *Thermodesulfovibrio*) (Fig. 5A). In parallel, the deltaproteobacterial Candidate Sva0485 clade, which is commonly detected in sulfate-reducing consortia (Kleindienst *et al.,* 2014; Bar-Or *et al.,* 2015), was relatively abundant in Lake Towuti sediments (Figs 3 and 5A). Although this clade has been found in a variety of environments and was often assumed to be reducing sulfate (Hori *et al.,* 2014; Concheri *et al.,* 2017), it has not been clearly reported to carry functional marker genes of sulfate reduction (Meyer and Kuever, 2007; Aoki *et al.,* 2015; Müller *et al.,* 2015) and it may be limited to fermentation (Plugge *et al.,* 2011; Kip *et al.,* 2017). Nevertheless, many of the *dsrAB* genes were recovered from various uncultivated Deltaproteobacteria (Supporting Information), which could include the Sva0485 clade listed in the 16S rRNA gene dataset (Fig. 3). In addition, taxonomic affiliations of the *asrA* and *phsA* genes demonstrated that members of the Deltaproteobacteria, Firmicutes and Chloroflexi, including few Nitrospirae and Bathyarchaeota, have the metabolic potential to reduce sulfite and thiosulfate (Fig. 5A). The substantial number of *hydB* gene sequences affiliated with Bathyarchaeota, Deltaproteobacteria and Chloroflexi also indicated metabolic potential for microbial reduction of ES or polysulfide.

The relative abundances of taxa related to bacteria known to reduce Fe in the laboratory (FeRB, Fig. 3) tended to exist throughout the sediment cores, successively appearing as *Deferrisoma*, *Geobacter*, *Thermincola, Geothrix* and *Anaeromyxobacter* (Figs 3 and 4). *Deferrisoma* species are known to reduce ferrihydrite, but also ES (Slobodkina *et al.,* 2012). *Geobacter* species are capable of Fe reduction in cultures, but are also known to participate as fermenters in syntrophic partnerships (Nagarajan *et al.,* 2013). *Thermincola* reduces ferrihydrite and magnetite, and also has the capacity to reduce sulfonates (Zavarzina *et al.,* 2007). Laboratory strains of *Geothrix* reduce various forms of soluble and insoluble Fe^{3+} via electron shuttles (Nevin and Lovley, 2002). *Anaeromyxobacter* couples the reduction of amorphous Fe^{3+} to the oxidation of acetate, but is also capable of a broad array of metabolic strategies (He and Sanford, 2003). Overall, our 16S rRNA gene sequences and functional marker gene sequences reveal a number of taxa related to microorganisms known to conduct sulfate reduction and Fe reduction in laboratory settings. These organisms and functional genes are broadly distributed throughout these sediments. Many of these organisms differed in relative abundance with depth below the water–sediment interface, implying community structuring that may be linked to the depth distributions of key substrates like sulfate, ferric Fe and OM. Although more detailed studies are needed to connect the metabolic potential of specific taxa to their role in biogeochemical processes, we speculate that many of them may have redundant modes of energy metabolism that allow facultative use of iron, sulfate and sulfur intermediates

(i.e. SO_3^{2-}, $S_2O_3^{2-}$, $S_2O_6^{2-}$, S_x^0) as substrates. This could be confirmed by the taxonomic distribution of the corresponding functional genes related to sulfur metabolism (i.e. *dsrAB*, *aprAB*, *asrA*, *phsA*, *hydB*) that is consistent with biochemical phenotypes predicted from the 16S rRNA phylogeny (Figs 4–5A and D).

The generation of sulfate via the re-oxidation of sulfide involves the formation of ES and a mixture of polysulfide and thionates (Santos *et al.,* 2015), which are subsequently microbially disproportionated to sulfide and sulfate to drive a cryptic sulfur cycle potentially stimulated by ferric iron and AOM processes with precipitation of pyrite in the sediment (Holmkvist *et al.,* 2011; Hansel *et al.,* 2015). The absence of AVS and trace amounts of ES in the sediment (Fig. 2) likely result from the metabolic capacity of extant microorganisms to reduce sulfate (*dsrAB*, *aprAB*) sulfite (*dsrAB*, *asrA*), thiosulfate (*phsA*) and polysulfide (*hydB*) (Fig. 5B and C). Although enzymatic pathways of ES disproportionation are not fully resolved yet, under anaerobic conditions, polysulfide could be microbially disproportionated via reversion of sulfate reduction, cleaving of thiosulfate and sulfite oxidoreductase (reverse *aprAB, phsA* and *asrA*), forming hydrogen sulfide via sulfur reductase (*hydB*) and sulfate via heterodisulfide reductase (*hdrA*) (Frederiksen and Finster, 2003; Osorio *et al.,* 2013; Santos *et al.,* 2015). Although, the metabolic potential to drive these reactions was detected, the rapid precipitation of Fe disulfides (i.e. CRS) in the sediment suggests that the recycling of Fe monosulfides and ES via sulfur disproportionation is restricted. Because polysulfide, thiosulfate and sulfite can serve as both electron donors and acceptors during reverse oxidation processes (Finster, 2011), sulfate reduction, methanogenesis and potentially iron reduction could still co-occur at extremely low pSRR in anoxic ferruginous sediments (Wang *et al.,* 2008). Microbial re-oxidation of HS^- was considered unlikely as the detection of *sox* and *SUOX* genes, which are involved in the aerobic oxidation of sulfur compounds (Ghosh and Dam, 2009), was minimal, their taxonomic assignments mainly pointing at taxa preserved from the water column (Supporting Information).

Potential for Syntrophy and Methanogenesis

Taxa related to known syntrophs were successively detected in the lower depths of the sediment including *Smithella* (Liu *et al.,* 1999)*, Syntrophothermus* (Sekiguchi *et al.,* 2000), *Pelospora* (Matthies *et al.,* 2000) and *Pelotomaculum* (Imachi *et al.,* 2002). This depth distribution of syntrophic taxa may also reflect substrate availability and notably a likely decrease in the availability of inorganic electron acceptors like SO_4^{2-} or Fe^{3+}. This is consistent with our observation at the deep site that when the relative abundance of 16S rRNA genes related to known SRB dropped below 10%, those of Ruminococcaceae and Clostridiales increased drastically (Fig. 3). Many taxa within these groups are known to interact syntrophically with both SRB and methanogens (Thauer *et al.,* 2008; Morris *et al.,* 2013). The distribution of acetate in pore water implies production of fermentation end products in the deeper sediments, which may also include hydrogen. Taxonomic affiliations of the *fhs* genes, which are a proxy for acetogenic microorganisms (Coolen and Orsi, 2015), pointed to Deltaproteobacteria, Firmicutes and Chloroflexi as the main producers of formate and acetate, whereas the *fdh* genes indicated that these products are mainly consumed by Deltaproteobacteria and not methanogens (Fig. 5A).

In uppermost sediments, taxa related to known methanogens were mainly affiliated with *Methanomassiliicoccus* (Figs 3 and 4). The *Methanomassiliicoccus* are known methylotrophs and thus use non-competitive substrates for methane production, such as methanol and maybe methylated thiols in sulfidogenic acetogenic associations (Plugge *et al.,* 2011; Dridi *et al.,* 2012; Kröninger *et al.,* 2016). Although not directly cross-checking the 16S taxonomy, the detection of *mtaB* and *mtsA* gene sequences confirmed the potential use of these substrates by Bathyarchaeota and Methanomicrobia (Fig. 5A). At both sites below 10 cmblf where pSRR were minimal (Fig. 2), the relative abundances of taxa affiliated with putative methanogens increased consisting mostly of sequences identified as Bathyarchaeota and *Candidatus* Methanofastidiosum, which were also recently considered to be able to carry out H_2-utilizing methylotrophic methanogenesis, with methane production mainly derived from the reduction of methylated compounds (Evans *et al.,* 2015; Nobu *et al.,* 2016). Identification of *mtbA* gene sequences affiliated with Bathyarchaeota and Methanomicrobia confirmed the potential use of methylamines as a substrate for methane production by these taxa (Fig. 5A). Nevertheless, the increasing abundance of hydrogen producers (e.g. Clostridiales and Ruminococcaceae) below 10 cmblf would support hydrogenotrophic methanogenesis as the main pathway for methane production at depth. The affiliation of a substantial number of *cdhA* gene sequences with Bathyarchaeota further suggested that members of this microbial phylum perform autotrophic methanogenesis (Sarmiento *et al.,* 2013; Lang *et al.,* 2015). Finally, taxonomy of the *mcrA* gene (i.e. methanogenesis, anaerobic methane oxidation) pointed to the role of Methanomicrobia and Methanobacteria in producing methane, and also reveal *mcrA* gene sequences affiliated with the Bathyarchaeota and ANME-1 (Fig. 5A). However, their degree of activity and the electron acceptor to which AOM processes are coupled remain undetermined.

Altogether, our data suggest that microbial communities in anoxic ferruginous sediments exhibit vertical

succession of the putative phenotypes FeRB, SRB, methanogens and methanotrophs (Fig. 5B), forming a microbial community different from those reported from lacustrine environments with ferruginous conditions in the pore water (Norði *et al.,* 2013; Bravo *et al.,* 2018). Although, the metabolic potential to reduce and disproportionate sulfur compounds was present, the absence of monosulfides and rapid increase of disulfides in the sediment suggested that cryptic sulfur cycling is minor, or even absent, compared to methanogenesis.

Experimental procedures

Sampling was performed at two locations, a shallow (60 m) and deep (200 m) site with oxic and anoxic bottom water conditions respectively (Fig. 1B). Oxygen concentrations in the water column were measured on site using a submersible Conductivity-Temperature-Depth probe (SBE-19, Sea-Bird). Additionally, several short sediment cores (< 50 cm) were retrieved at each site. To avoid oxidation, all sediment sampling and processing was carried out on site inside a nitrogen-filled glove bag. Pore water was extracted using Rhizon Pore Water Samplers (Rhizon CSS), collected in syringes and filtered (0.2 μm pore size).

Pore water chemistry, sulfate reduction rates, Total reduced inorganic sulfur

Dissolved Fe^{2+} concentrations in pore water were measured in the field via spectrophotometry (Viollier *et al.,* 2000) by adding 100 μl of Ferrozine Iron Reagent (Sigma-Aldrich) to 1 ml of pore water and measuring absorbance of the coloured solution at 562 nm with a DR 3900 spectrophotometer (Hach). Detection limit of the method is 0.25 μM. Sulfate, acetate and formate concentrations were analysed in the home lab by suppressed ion chromatography. The system consisted of a S5200 sample injector, a S3115 conductivity detector and a 4.0 × 150 mm LCA A20 column (all Sykam) and a SeQuant SAMS anion IC suppressor (EMD Millipore). Eluent composition was 1.7 mM $NaHCO_3$ and 1.8 mM Na_2CO_3 and flow rate was set to 1 ml min^{-1} and column temperature to 45°C. Respective minimum detection (Signal to Noise ratio = 3) and quantification limits (S/N = 10) are: SO_4^{2-} (2 μM; 8.4 μM), formate (2.1 μM; 8 μM) and acetate (8.7 μM; 27.1 μM). Standards were run every ten samples. Reproducibility was always below 3%.

Potential SRR quantification was performed according to the whole core incubation technique of Jørgensen (1978). In brief, 3 kBq of $^{35}SO_4^{2-}$ radiotracer were injected into each sediment plug and incubated for 24 h in the dark close to *in situ* temperature (ca. 30°C) followed by cold chromium distillation (Kallmeyer *et al.,* 2004). Radioactivity was quantified using UltimaGold Scintillation Cocktail (Perkin Elmer) and a Tri Carb 2500 TR liquid scintillation counter (Packard Instruments) with a counting window of 4–167 keV. Detailed protocols are published elsewhere (Vuillemin *et al.,* 2016).

Concentrations of TRIS compounds were determined separately from the pSRR incubations, using approximately 5 g of fresh sediment per sample. Sediment samples were distilled following a modification of the procedure by Canfield *et al*. (1986) and Kallmeyer *et al*. (2004). During the three steps of distillation, TRIS was separated into three fractions, namely AVS, CRS and ES. All three fractions were extracted in three successive 2 h distillation steps, consecutively adding 8 ml of 6 N HCl (AVS), 16 ml of 1 M $CrCl_2$ solution (CRS) and 8 ml of dimethylformamide (ES) to the sample (Kallmeyer *et al.,* 2004). Sample slurries were stirred in a glass flask under a continuous stream of nitrogen gas. The liberated hydrogen sulfide was trapped in 7 ml of 5% (w/v) zinc acetate solution to precipitate as zinc sulfide. After each distillation cycle, the zinc acetate solution was exchanged for a fresh one. The trapping solution was centrifuged, the supernatant discarded and the ZnS pellet suspended in 1 ml of ultrapure H_2O. Sulfide concentrations in the final 1 ml suspensions obtained for each TRIS fraction were measured spectrophotometrically at 667 nm using Cline reagent (Cline, 1969) and a DR 3900 spectrophotometer (Hach). Minimum detection limit of this method is 5 μg L^{-1}. Samples were processed in duplicates, and concentrations were averaged with error bars corresponding to one standard deviation.

General geochemical data were presented and discussed in detail in a previous study (Vuillemin *et al.,* 2016). The corresponding dataset is archived on the Pangaea® database (www.pangaea.de/) under accession number # 861437.

Intracellular DNA extraction

The procedure of Alawi *et al*. (2014) allows for the separate extraction of extracellular DNA (eDNA) and iDNA from the same sample. To specifically analyse the current microbial communities of the sediment, we only used the iDNA fraction in this study. All extractions were performed in duplicates along with a negative control. The first part of the extraction was performed with 1.0 g of fresh sediment, 0.2 g of acid washed polyvinylpolypyrrolidone and 2.5 ml of 0.1 M sodium phosphate buffer (Na-P-buffer). The sediment was washed three times with Na-P-buffer and the supernatant of all washing steps retrieved and pooled, reaching a final volume of 7.5 ml. This supernatant was centrifuged for 45 min at 4700 × g to separate the iDNA (i.e. cell pellet) from the eDNA (i.e. supernatant). The iDNA fraction was extracted from

the cell pellet following our previously published protocol (Vuillemin *et al.,* 2017). For further analysis, we selected iDNA samples in duplicates from four different sediment depths at each coring site (shallow site: 0.5, 7.5, 15, 27.5 cmblf; deep site: 1.5, 7.5, 15, 32.5 cmblf). Final extracts were diluted 10 times and used as templates in PCR reactions.

Quantitative PCR assays

Quantitative PCR was performed on eight iDNA extracts using primer pairs specifically targeting the bacterial 16S rRNA gene, methyl coenzyme M reductase alpha subunit (*mcrA*) and dissimilatory sulfite reductase beta subunit (*dsrB*) genes. For each 20 μl reaction unit, PCR mixtures were composed of 10 μl of iTaq SYBR Green Supermix (Bio-Rad), 0.1 μl of each of the primers (100 μM), 7.8 μl of Ultra-pure PCR Water (Bioline) and 2 μl of DNA template diluted 10 times. Samples were processed in triplicate with six standards at increasing dilutions from 1 to 1×10^6 times. Negative controls were added to all PCR sets with 2 μl of Ultra-pure PCR Water (Bioline) as template to provide a contamination check. Positive controls were also added using 2 μl of *Escherichia coli*, *Methanosarcina barkeri* and *Desulfovibrio vulgaris* (0.1 ng μL^{-1}), respectively. PCR reactions were run on a CFX Connect Real-Time System thermocycler (Bio-Rad).

For bacterial 16S rRNA gene, we used primer pairs Eub341F (5′- CCT ACG GGA GGC AGC AG -3′) with Eub534R (5′- ATT ACC GCG GCT GCT GG -3′) with an initial standard concentration of 2.3×10^7 gene copies μL^{-1}. PCR cycles were run as follows: Initial denaturation of 5 min at 98°C, 40 cycles of 98°C for 5 s, 58°C for 20 s, 72°C for 50 s, with a final melting curve of 95°C for 10 s, 65°C for 5 s incremented by 0.5°C per cycle of 5 s to reach 95°C. For the *mcrA* gene, the primer pair was msla-F (5′- GGT GGT GTM GGD TTC ACM CAR TA-3′) with mcrA-R (5′- CGT TCA TBG CGT AGT TVG GRT AGT -3′) with an initial standard concentration of 1.6×10^7 gene copies μL^{-1}. For the *dsrB* gene, we used the primer pair dsrB4-R (5′-GTG TAG CAG TTA CCG CA -3′) with dsrB2060-F (5′- CAA CAT CGT YCA YAC CCA GGG-3′) with an initial standard concentration of 6.69×10^7 gene copies μl^{-1}. For both primer combinations, PCR cycles were run as follows: Initial denaturation of 3 min at 95°C, 40 cycles of 95°C for 30 s, 60°C for 20 s, 72°C for 30 s plus 80°C for 3 s, with a final melting curve of 65°C for 5 s incremented by 0.5°C per cycle of 5 s to reach 95°C.

Run efficiencies for the quantification of the bacterial 16S rRNA gene, *mcrA* and *dsrB* were 97.5%, 75.0% and 92.7% respectively, with correlation coefficient slope between 0.997 and 0.999. All final products were checked on 1.5% agarose gels.

PCR amplification for next-generation sequencing

PCR was performed on 16 iDNA extracts using unique combinations of the tagged universal primer pair 515F (5′- GTG CCA GCM GCC GCG GTA A -3′) and 806R (5′- GGA CTA CHV GGG TWT CTA AT -3′) to cover 291 bp of the bacterial and archaeal 16S rRNA gene. We acknowledge that this primer pair does not include the adaptation for increased coverage of archaea (Parada *et al.,* 2016). Individual tags composed of eight nucleotides were attached at each primer 5′-end. A total of 20 different forward and reverse tagged primers (Eurofins Genomics) were designed to enable multiplexing of all PCR products in a unique sequencing library. PCR mixtures were prepared and amplifications performed as previously published (Vuillemin *et al.,* 2017). PCR amplicons were checked on 1.5% agarose gel. For each sample, 116 μl of PCR product were pooled, purified and eluted in a final volume of 25 μl, using a High Pure PCR Cleanup Micro Kit (Roche Applied Science). Purified PCR products were quantified by fluorometric method using a QubitHS dsDNA kit (Invitrogen). Concentrations were calculated and normalized for all samples. We pooled 32 ng of each DNA amplicon sample and reduced the volume of the mixture to 120 μl using a Savant SpeedVac High Capacity Concentrator (Thermo Fisher Scientific). We used 60 μl of pooled amplicons, corresponding to an amount of approximately 800 ng of DNA, for the Illumina MiSeq library preparation.

Illumina library preparation, sequencing and data analysis

Indexed paired-end libraries of pooled amplicons for consecutive cluster generation and DNA sequencing were constructed using a TruSeq DNA PCR-Free L Kit (Illumina). Libraries were prepared following the manufacturer instructions. PCR-free libraries were validated by qPCR using the KAPA Library Quantification Kit (Kapa Biosystems) following the manufacturer's manual. PCR mixtures were prepared and amplifications performed as previously published (Vuillemin *et al.,* 2017). Final concentration of the library was quantified by a fluorometric method using a Qubit HS dsDNA kit (Invitrogen). A MiSeq Reagent Nano kit v2, with 500 cycles with nano (2 tiles) flow cells was used to run libraries on the Illumina MiSeq Sequencing System. Two 250 cycles were used for an expected output of 500 Mb and an expected number of 7 million reads per library.

Quality of the raw data was checked using FastQC. Demultiplexing was performed using own scripts based on cutadapt (Martin, 2011). No errors in barcodes were allowed with Phred-Score above Q25. Read pairs were

merged using PEAR (Zhang *et al.,* 2014). Sequences were trimmed using Trimmomatic (Bolger *et al.,* 2014). Chimeras were detected and removed using usearch61 and the ChimeraSlayer reference database (Edgar, 2010) as it is implemented in the QIIME-pipeline (Caporaso *et al.,* 2010). Script of this pipeline was used to cluster the sequences and assign taxonomies based on the SILVA 16S rRNA SSU NR99 reference database release 128 (Quast *et al.,* 2013) at 97% identity cut-off value (DeSantis *et al.,* 2006). The resulting operational taxonomic unit (OTU) table was filtered by removing all OTUs with abundance below 0.1% within the sample. Those affiliated with cultivated SRB, FeRB, syntrophs involved in hydrogen production and transfer, methanogens and anaerobic methanotrophs as well as uncultivated clades with the same inferences from single-cell and metagenomic studies were selected to plot bar charts of the corresponding phenotypes (Fig. 3). Relative abundances were calculated by dividing their respective number of reads by the total number of reads per sample. Percentages of relative abundance were summed up by duplicates and averaged.

Sequencing data after demultiplexing were submitted to the European Nucleotide Archive (http://www.ebi.ac.uk/ena) under study accession number PRJEB14484.

Phylogenetic analysis and canonical correspondence analysis

Representative sequences extracted for all OTUs plotted in the bar charts (Fig. 3) were aligned to the SILVA database and plotted in four different phylogenetic trees, that is, Deltaproteobacteria (Fig. 4A), Archaea (Fig. 4B), Acidobacteria and Nitrospirae including the Candidate NC10 (Fig. 4C) and Firmicutes (Fig. 4D). The SINA online v.1.2.11 (Pruesse *et al.,* 2007, 2012) was used to align our representative sequences. Phylogenetic analysis was performed with ARB software package (Ludwig *et al.,* 2004) based on the upload sequence alignments against the SILVA 16S rRNA SSU NR99 reference database release 128 (Quast *et al.,* 2013). Their closest environmental sequences and cultured species were selected as taxonomic references and used to calculate phylogenetic trees with nearly full-length sequences (> 1400 bp) using the implemented bacterial and archaeal filter and the Maximum Likelihood algorithm RAxML with advanced bootstrap refinement using 100 tree replicates (Stamatakis, 2006). Partial sequences were added to the tree using the maximum parsimony algorithm without allowing changes of tree topology. Each phylogenetic tree included representative sequences from Lake Towuti and their respective reference sequences for Archaea, Deltaproteobacteria, Firmicutes as well as Acidobacteria together with Nitrospirae. The same procedure was applied to assign all unassigned sequences, which we then implemented in the initial OTU table.

In addition, a CCA was performed with 12 environmental parameters as explanatory variables and all OTUs corresponding to the different selected metabolic pathways (i.e. 204 OTUs). Explanatory variables were standardized prior to computation. The CCA was run using the Past 3.10 software (Hammer *et al.,* 2001). Significance of canonical axes was tested via permutation computed for N = 999. Results are available as Supporting Information.

Metagenomic libraries and taxonomic identification of functional genes

Two iDNA samples (S site: 27.5 cmblf; D site: 32.5 cmblf) were sent to the DOE Joint Genome Institute (JGI, Walnut Creek, CA) for metagenomic sequencing and assembling (Chin *et al.,* 2013). Samples received accession number I17A3 metaG (project ID: 1107606) and I19B2 metaG (project ID: 1107610) and are included in the Microbial Dark Matter project (proposal ID: 1477). Metagenomic data were obtained via second and third generation high throughput sequencing platforms. Structural and functional annotation was carried out through the JGI's Microbial Genome Annotation Pipeline (MGAP v. 4) as described in Huntemann *et al*. (2015). Assembled metagenomic data were screened on the JGI Genome portal IMG/M (http://genome.jgi.doe.gov/) and predicted protein sequences of formate-tetrahydrofolate ligase (*fhs*), formate dehydrogenase (*fdh*), dissimilatory sulfite reductase alpha and beta subunits (*dsrAB*), adenylylsulfate reductase alpha and beta subunits (*aprAB*), anaerobic sulfite reductase alpha subunit (*asrA*), thiosulfate/polysulfide reductase alpha subunit (*phsA*), sulfhydrogenase or sulfur reductase beta subunit (*hydB*), sulfur-oxidizing protein multiple subunits (*soxBCDXY*), sulfite oxidase (*SUOX*), methyl-coenzyme M reductase alpha to gamma subunits (*mcrA*), methanol coenzyme M methyltransferase beta subunit (*MtaB*), methylamine-specific coenzyme M methyltransferase alpha subunit (*MtbA*), methylthiol coenzyme M methytransferase alpha subunit (*mtsA*), carbon-monoxide dehydrogenase (*CODH*), acetyl-CoA decarbonylase alpha subunit (*cdhA*), tetrahydromethanopterin S-methyltransferase alpha subunit (*mtrA*), and heterodisulfide reductase alpha subunit (*hdrA*) were exported for taxonomic identification.

Protein encoding genes and ORFs were assigned to high-level taxonomic groups (class level and above) using PhymmBL (Brady and Salzberg, 2009). The interpolated Markov model (IMM) bacterial and archaeal database was implemented with genomes available in the NCBI RefSeq database and JGI database, using the customGenomicData.pl script available with the PhymmBL

download. Taxonomic identifications were integrated with the functional annotations performing BLASTp searches of ORFs against the SEED database, as described previously (Orsi *et al.,* 2013, 2017).

Acknowledgements

This study was financially and logistically supported by the ICDP priority program of the Deutsche Forschungsgemeinschaft (DFG Schwerpunktprogramm) through grants to Jens Kallmeyer (KA 2293/8-1), Aurèle Vuillemin (VU 94/1-1) and William Orsi (OR 417/1-1); the Swiss National Science Foundation (SNSF grant no. P2GEP2_148621 to Aurèle Vuillemin); the Helmholtz Center Potsdam, German Research Center for Geoscience (GFZ); and an NSERC Discovery grant (no. 0487) to Sean A. Crowe.

We thank Tri Widiyanto and his staff from the Indonesia Research Center for Limnology for their administrative support in obtaining the Scientific Research Permit. Jan Axel Kitte, Carriayne Jones, Sulung Nomosatryo and Céline C.P. Michiels are thanked for their assistance during sampling at Lake Towuti, and PT Vale Indonesia for field support. The supervision during Illumina Miseq procedure of Jan Pawlowski, Maria Holzmann, Laure Perret-Gentil, Emanuela Reo and their research partners at the University of Geneva (Switzerland) are kindly acknowledged. Florian Schubert is thanked for processing the samples for total reduced inorganic sulfur analysis.

References

Alawi, M., Schneider, B., and Kallmeyer, J. (2014) A procedure for separate recovery of extra- and intracellular DNA from a single marine sediment sample. *J Microbiol Meth* **104**: 36–42.

Aoki, M., Kakiuchi, R., Yamaguchi, T., Takai, K., Inagaki, F., and Imachi, H. (2015) Phylogenetic diversity of *apr*A genes in subseafloor sediments on the northwestern Pacific margin off Japan. *Microbes Environ* **30**: 276–280.

Bar-Or, I., Ben-Dov, E., Kushmaro, A., Eckert, W., and Sivan, O. (2015) Methane-related changes in prokaryotes along geochemical profiles in sediments of Lake Kinneret (Israel). *Biogeosciences* **12**: 2847–2860.

Beal, E. J., House, C. H., and Orphan, V. J. (2009) Manganese and iron-dependent marine methane oxidation. *Science* **325**: 184–187.

Boetius, A., Ravenschlag, K., Schubert, C. J., Rickerts, D., Widdel, F., Gieseke, A., *et al*. (2000) A marine microbial consortium apparently mediating anaerobic oxidation of methane. *Nature* **407**: 623–626.

Bolger, A. M., Lohse, M., and Usadel, B. (2014) Trimmomatic: a flexible trimmer for Illumina sequence data. *Bioinformatics* **30**: 2114–2120.

Brady, A., and Salzberg, S. L. (2009) Phymm and PhymmBL: metagenomic phylogenetic classification with interpolated Markov models. *Nat Methods* **6**: 673–676.

Bramburger, A. J., Hamilton, P. B., Hehanussa, P. E., and Haffner, G. D. (2008) Processes regulating the community composition and relative abundance of taxa in the diatom communities of the Malili Lakes, Sulawesi Island, Indonesia. *Hydrobiologia* **615**: 215–224.

Bravo, A. G., Zopfi, J., Buck, M., Xu, J., Bertilsson, S., Schaefer, J. K., *et al*. (2018) *Geobacteraceae* are important members of mercury-methylating microbial communities of sediments impacted by waste water releases. *ISME J* **12**: 802–812.

Canfield, D. E., Raiswell, R., Westrich, J. T., Reaves, C. M., and Berner, R. A. (1986) The use of chromium reduction in the analysis of reduced inorganic sulfur compounds in sediments and shales. *Chem Geol* **54**: 149–155.

Canfield, D. E., Stewart, F. J., Thamdrup, B., De Brabandere, L., Dalsgaard, T., Delong, E. F., *et al*. (2010) A cryptic sulfur cycle in oxygen minimum zone waters off the Chilean coast. *Science* **330**: 1375–1378.

Caporaso, J. G., Kuczynski, J., Stombaugh, J., Bittinger, K., Bushman, F. D., Costello, E. K., *et al*. (2010) QIIME allows analysis of high-throughput community sequencing data. *Nat Methods* **7**: 335–336.

Castro, H. F., Williams, N. H., and Ogram, A. (2000) Phylogeny of sulfate-reducing bacteria. *FEMS Microbiol Ecol* **31**: 1–9.

Chin, C.-S., Alexander, D. H., Marks, P., Klammer, A. A., Drake, J., Heiner, C., *et al*. (2013) Nonhybrid, finished microbial genome assemblies from long-read SMRT sequencing data. *Nat Methods* **10**: 563–569.

Cline, J. D. (1969) Spectrophotometric determination of hydrogen sulfide in natural waters. *Limnol Oceanogr* **14**: 454–458.

Concheri, G., Stevanato, P., Zaccone, C., Shotyk, W., D'Orazio, V., Miano, T., *et al*. (2017) Rapid peat accumulation favours the occurrence of both fen and bog microbial communities within a Mediterranean, free-floating peat island. *Sci Rep UK* **7**: 8511.

Coolen, M. J. L., and Orsi, W. D. (2015) The transcriptional response of microbial communities in thawing Alaskan permafrost soils. *Front Microbiol* **6**: 197.

Costa, K. M., Russell, J. M., Vogel, H., and Bijaksana, S. (2015) Hydrological connectivity and mixing of Lake Towuti, Indonesia, in response to paleoclimatic changes over the last 60,000 years. *Palaeogeogr Palaeocl* **417**: 467–475.

Crowe, S. A., Pannalal, S. J., Fowle, D. A., Cioppa, M. T., Symons, D. T. A., Haffner, G. D., and Fryer, B. J. (2004) Biogeochemical cycling in Fe-rich sediments from Lake Matano. *Indonesia Int Symp Water Rock Interact* **11**: 1185–1189.

Crowe, S. A., Katsev, S., Hehanussa, P., Haffner, G. D., Sundby, B., Mucci, A., and Fowle, D. A. (2008a) The biogeochemistry of tropical lakes: a case study from Lake Matano, Indonesia. *Limnol Oceanogr* **53**: 319–331.

Crowe, S. A., Jones, C. A., Katsev, S., Magen, C., O'Neill, A., Sturm, A., *et al*. (2008b) Photoferrotrophs thrive in an Archean Ocean analogue. *Proc Natl Acad Sci USA* **105**: 15938–15943.

Crowe, S. A., Katsev, S., Leslie, K., Sturm, A., Magen, C., Nomosatryo, S., *et al*. (2011) The methane cycle in ferruginous Lake Matano. *Geobiology* **9**: 61–78.

DeSantis, T. Z., Hugenholtz, P., Larsen, N., Rojas, M., Brodie, E. L., Keller, K., *et al*. (2006) Greengenes, a chimera-checked 16S rRNA gene database and

workbench compatible with ARB. *Appl Environ Microb* **72**: 5069–5072.

Dridi, B., Fardeau, M. L., Ollivier, B., Raoult, D., and Drancourt, M. (2012) *Methanomassiliicoccus luminyensis* gen. Nov., sp. nov., a methanogenic archaeon isolated from human faeces. *Int J Syst Evol Microbiol* **62**: 1902–1907.

Edgar, R. C. (2010) Search and clustering orders of magnitude faster than BLAST. *Bioinformatics* **26**: 2460–2461.

Ettwig, K. F., Zhu, B., Speth, D., Keltjens, J. T., Jetten, M. S., and Kartal, B. (2016) Archaea catalyze iron-dependent anaerobic oxidation of methane. *Proc Natl Acad Sci USA* **113**: 12792–12796.

Evans, P. N., Parks, D. H., Chadwick, G. L., Robbins, S. J., Orphan, V. J., Golding, S. D., and Tyson, G. W. (2015) Methane metabolism in the archaeal phylum Bathyarchaeota revealed by genome-centric metagenomics. *Science* **350**: 434–438.

Finster, K. (2011) Microbiological disproportionation of inorganic sulfur compounds. *J Sulfur Chem* **29**: 281–292.

Frederiksen, T.-M., and Finster, K. (2003) Sulfite-oxido-reductase is involved in the oxidation of sulfite in *Desulfocapsa sulfoexigens* during disproportionation of thiosulfate and elemental sulfur. *Biodegradation* **14**: 189–198.

Greene, A. C. (2014)The family Desulfuromonadaceae . In *The Prokaryotes*, Rosenberg, E., DeLong, E. F., Lory, S., Stackebrandt, E., and Thompson, F. (eds). Berlin, Germany: Springer, pp. 143–155.

Ghosh, W., and Dam, B. (2009) Biochemistry and molecular biology of lithotrophic sulfur oxidation by taxonomically and ecologically diverse bacteria and archaea. *FEMS Microbiol Rev* **33**: 999–1043.

Haffner, G. D., Hehanussa, P. E., and Hartoto, D. (2001)The biology and physical processes of large lakes of Indonesia: lakes Matano and Towuti . In *The Great Lakes of the World (GLOW): Food-Web, Health, and Integrity*, Munawar, M., and Hecky, R. E. (eds). Leiden: Blackhuys, pp. 183–194.

Hammer, Ø., Harper, D. A. T., and Ryan, P. D. (2001) PAST: paleontological statistics software package for education and data analysis. *Palaeontol Electron* **4**: 1–9.

Hansel, C. M., Lentini, C. J., Tang, Y., Johnston, D. T., Wankel, S. D., and Jardine, P. M. (2015) Dominance of sulfur-fueled iron oxide reduction in low-sulfate freshwater sediments. *ISME J* **9**: 2400–2412.

He, Q., and Sanford, R. A. (2003) Characterization of Fe(III) reduction by chlororespiring *Anaeromyxobacter dehalogenans*. *Appl Environ Microbiol* **69**: 2712–2718.

He, Z., Geng, S., Cai, C., Liu, S., Liu, Y., Pan, Y., *et al*. (2015) Anaerobic oxidation of methane coupled to nitrite reduction by halophilic marine NC10 bacteria. *Appl Environ Microb* **81**: 5538–5545.

Holmkvist, L., Ferdelman, T. G., and Jørgensen, B. B. (2011) A cryptic sulfur cycle driven by iron in the methane zone of marine sediment (Aarhus Bay, Denmark). *Geochim Cosmochim Acta* **75**: 3581–3599.

Hori, T., Kimura, M., Aoyagi, T., Navarro, R. R., Ogata, A., Sakoda, A., *et al*. (2014) Biodegradation potential of organically enriched sediments under sulfate- and iron-reducing conditions as revealed by the 16S rRNA deep sequencing. *J Water Environ Tech* **12**: 357–366.

Huntemann, M., Ivanova, N. N., Mavromatis, K., Tripp, H. J., Paez-Espino, D., Palaniappan, K., *et al*. (2015) The standard operating procedure of the DOE-JGI microbial genome annotation pipeline (MGAP v. 4). *Stand Genomic Sci* **10**: 86.

Imachi, H., Sekiguchi, Y., Kamagata, Y., Hanada, S., Ohashi, A., and Harada, H. (2002) *Pelotomaculum thermopropionicum* gen. Nov., sp. nov., an anaerobic, thermophilic, syntrophic propionate-oxidizing bacterium. *Int J Syst Evol Microbiol* **52**: 1729–1735.

Jørgensen, B. B. (1978) A comparison of methods for the quantification of bacterial sulfate reduction in coastal marine sediments. I. Measurements with radiotracer techniques. *Geomicrobiol J* **1**: 11–27.

Kaksonen, A. H., Spring, S., Schumann, P., Kroppenstedt, R. M., and Puhakka, J. A. (2007) *Desulfurispora thermophile* gen. Nov., sp. nov., a thermophilic, spore-forming sulfate-reducer isolated from a sulfidogenic fluidized-bed reactor. *Int J Syst Evol Microbiol* **57**: 1089–1094.

Kallmeyer, J., Ferdelman, T. G., Weber, A., Fossing, H., and Jørgensen, B. B. (2004) A cold chromium distillation procedure for radiolabeled sulfide applied to sulfate reduction measurements. *Limnol Oceanogr Meth* **2**: 171–180.

Katsev, S., Crowe, S. A., Mucci, A., Sundby, B., Nomosatryo, S., Haffner, G. D., and Fowle, D. A. (2010) Mixing and its effects on biogeochemistry in the persistently stratified, deep, tropical Lake Matano, Indonesia. *Limnol Oceanogr* **55**: 763–776.

Kip, N., Jansen, S., Leite, M. F. A., de Hollander, M., Afanasyev, M., Kuramae, E. E., and Van Veen, J. A. (2017) Methanogens predominate in natural corrosion protective layers on metal sheet piles. *Sci Rep UK* **7**: 11899.

Kleindienst, S., Herbst, F.-A., Stagars, M., von Netzer, F., von Bergen, M., Seifert, J., *et al*. (2014) Diverse sulfate-reducing bacteria of hdrAthe Desulfosarcina/Desulfococcus clade are the key alkane degraders at marine seeps. *The ISME J* **8**: 2029–2044.

Kröninger, L., Berger, S., Welte, C., and Deppenmeier, U. (2016) Evidence for the involvement of two heterodisulfide reductases in the energy-conserving system of *Methanomassiliicoccus luminyensis*. *FEBS J* **283**: 472–483.

Lang, K., Schuldes, J., Klingl, A., Poehlein, A., Daniel, R., and Brune, A. (2015) New mode of energy metabolism in the seventh order of methanogens as revealed by comparative genome analysis of " *Candidatus* Methanoplasma termitum". *Appl Environ Microb* **81**: 1338–1352.

Langille, M. G. I., Zaneveld, J., Caporaso, J. G., McDonald, D., Knights, D., Reyes, J. A., *et al*. (2013) Predictive functional profiling of microbial communities using 16S rRNA marker gene sequences. *Nat Biotechnol* **31**: 814–823.

Liu, Y., Balkwill, D. L., Aldrich, H. C., Drake, G. R., and Boone, D. R. (1999) Characterization of the anaerobic propionate-degrading syntrophs *Smithella propionica* gen. Nov., sp. nov. and *Syntrophobacter wolinii*. *Int J Syst Bacteriol* **49**: 545–556.

Louca, S., Parfrey, L. W., and Doeblei, M. (2016) Decoupling function and taxonomy in the global ocean microbiome. *Science* **353**: 1272–1277.

Ludwig, W., Strunk, O., Westram, R., Richter, L., Meier, H., Yadhukumar, *et al*. (2004) ARB: a software environment for sequence data. *Nucleic Acids Res* **32**: 1363–1371.

Martin, M. (2011) Cutadapt removes adapter sequences from high-throughput sequencing reads. *EMBnet J* **17**: 10–12.

Matthies, C., Springer, N., Ludwig, W., and Schink, B. (2000) *Pelospora glutarica* gen. Nov., sp. nov., a glutarate-fermenting, strictly anaerobic, spore-forming bacterium. *Int J Syst Evol Microbiol* **50**: 645–648.

Meyer, B., and Kuever, J. (2007) Molecular analysis of the diversity of sulfate-reducing and sulfur-oxidizing prokaryotes in the environment, using *aprA* as functional marker gene. *Appl Environ Microbiol* **73**: 7664–7679.

Meyerdierks, A., Kube, M., Kostadinov, I., Teeling, H., Glöckner, F. O., Reinhardt, R., and Amann, R. (2010) Metagenome and mRNA expression analyses of anaerobic methanotrophic archaea of the ANME-1 group. *Environ Microbiol* **12**: 422–439.

Milucka, J., Ferdelman, T. G., Polerecky, L., Franzke, D., Wegener, G., Schmid, M., *et al*. (2012) Zero valent sulphur is a key intermediate in marine methane oxidation. *Nature* **491**: 541–546.

Morris, B. E. L., Henneberger, R., Huber, H., and Moissl-Eichinger, C. (2013) Microbial syntrophy: interaction for the common good. *FEMS Microbiol Rev* **37**: 384–406.

Müller, A. L., Kjeldsen, K. U., Rattei, T., Pester, M., and Loy, A. (2015) Phylogenetic and environmental diversity of DsrAB-type dissimilatory (bi)sulfite reductases. *ISME J* **9**: 1152–1165.

Nagarajan, H., Embree, M., Rotaru, A.-E., Shrestha, P. M., Feist, A. M., Palsson, B. Ø., *et al*. (2013) Characterization and modeling of interspecies electron transfer mechanisms and microbial community dynamics of a syntrophic association. *Nat Commun* **4**: 1–10.

Nevin, K. P., and Lovley, D. R. (2002) Mechanisms for accessing insoluble Fe(III) oxide during dissimilatory Fe(III) reduction by *Geothrix fermentans*. *Appl Environ Microb* **68**: 2294–2299.

Nobu, M. K., Narihiro, T., Kuroda, K., Mei, R., and Liu, W.-T. (2016) Chasing the elusive Euryarchaeota class WSA2: genomes reveal a uniquely fastidious methyl-reducing methanogen. *ISME J* **10**: 2478–2487.

Norði, K. A., Thamdrup, B., and Schubert, C. J. (2013) Anaerobic oxidation of methane in an iron-rich Danish freshwater lake sediment. *Limnol Oceanogr* **58**: 546–554.

Orsi, W. D., Edgcomb, V. P., Christman, G. D., and Biddle, J. F. (2013) Gene expression in the deep biosphere. *Nature* **499**: 205–208.

Orsi, W. D., Coolen, M. J. L., Wuchter, C., He, L., More, K. D., Irigoien, X., *et al*. (2017) Climate oscillations reflected within the microbiome of Arabian Sea sediments. *Sci Rep UK* **7**: 6040.

Osorio, H., Mangold, S., Denis, Y., Nancucheo, I., Esparza, M., Johson, B. D., *et al*. (2013) Anaerobic sulfur metabolism coupled to dissimilatory iron reduction in the extremophile *Acidithiobacillus ferrooxidans*. *Appl Environ Microb* **79**: 2172–2181.

Oude Elferink, S. J. W. O., Akkermans-van Vliet, W. M., Bogte, J. J., and Stams, A. J. M. (1999) *Desulfobacca acetoxidans* gen. Nov., sp. nov., a novel acetate-degrading sulfate reducer isolated from sulfidogenic granular sludge. *Int J Syst Bacteriol* **49**: 345–350.

Parada, A. E., Needham, D. M., and Fuhrman, J. A. (2016) Every base matters: assessing small subunit rRNA primers for marine microbiomes with mock communities, time series and global field samples. *Environ Microbiol* **18**: 1403–1414.

Pjevac, P., Kamyshny, A., Jr., Dyksma, S., and Mussmann, M. (2014) Microbial consumption of zero-valence sulfur in marine benthic habitats. *Environ Microbiol* **16**: 3416–3430.

Plugge, C. M., Zhang, W., Scholten, J. C. M., and Stams, A. J. M. (2011) Metabolic flexibility of sulfate-reducing bacteria. *Front Microbiol* **2**: 81.

Poulton, S. W., and Canfield, D. E. (2011) Ferruginous conditions: a dominant feature of the ocean through Earth's history. *Elements* **7**: 107–112.

Pruesse, E., Quast, C., Knittel, K., Fuchs, B. M., Ludwig, W., Peplies, J., and Glöckner, F. O. (2007) SILVA: a comprehensive online resource for quality checked and aligned ribosomal RNA sequence data compatible with ARB. *Nucleic Acids Res* **35**: 7188–7196.

Pruesse, E., Peplies, J., and Glöckner, F. O. (2012) SINA: accurate high-throughput multiple sequence alignment of ribosomal RNA genes. *Bioinformatics* **28**: 1823–1829.

Quast, C., Pruesse, E., Yilmaz, P., Gerken, J., Schweer, T., Yarza, P., *et al*. (2013) The SILVA ribosomal RNA gene database project: improved data processing and web-based tools. *Nucleic Acids Res* **41**: D590–D596.

Ramamoorthy, S., Sass, H., Langner, H., Schumann, P., Kroppenstedt, R. M., Spring, S., *et al*. (2006) *Desulfosporosinus lacus* sp. nov., a sulfate-reducing bacterium isolated from pristine freshwater lake sediments. *Int J Syst Evol Microbiol* **56**: 2729–2736.

Russell, J. M., Bijaksana, S., Vogel, H., Melles, M., Kallmeyer, J., Ariztegui, D., *et al*. (2016) The Towuti drilling project: paleoenvironments, biological evolution, and geomicrobiology of a tropical Pacific lake. *Sci Dri* **21**: 29–40.

Santos, A. A., Venceslau, S. S., Grein, F., Leavitt, W. D., Dahl, C., Johnston, D. T., and Pereira, I. A. C. (2015) A protein trisulfide couples dissimilatory sulfate reduction to energy conservation. *Science* **350**: 1541–1545.

Sarmiento, F., Mrázek, J., and Whitman, W. B. (2013) Genome-scale analysis of gene function in the hydrogenotrophic methanogenic archaeon *Methanococcus maripaludis*. *Proc Natl Acad Sci USA* **110**: 4726–4731.

Sekiguchi, Y., Kamagata, Y., Nakamura, K., Ohashi, A., and Harada, H. (2000) *Syntrophothermus lipocalidus* gen. Nov., sp. nov., a novel thermophilic, syntrophic, fatty-acid-oxidizing anaerobe which utilizes isobutyrate. *Int J Syst Evol Microbiol* **50**: 771–779.

Sekiguchi, Y., Muramatsu, M., Imachi, H., Narihiro, T., Ohashi, A., Harada, H., *et al*. (2008) *Thermodesulfovibrio aggregans* sp. nov. and *Thermodesulfovibrio thiophilus* sp. nov., anaerobic,thermophilic, sulfate-reducing bacteria isolated from thermophilic methanogenic sludge, and emended description of the genus *Thermodesulfovibrio*. *Int J Syst Evol Microbiol* **58**: 2541–2548.

Sieber, J. R., McInerney, M. J., and Gunsalus, R. P. (2012) Genomic insights into syntrophy: the paradigm for anaerobic metabolic cooperation. *Annu Rev Microbiol* **66**: 429–452.

Sivan, O., Adler, M., Pearson, A., Gelman, F., Bar-Or, I., John, S. G., and Eckert, W. (2011) Geochemical evidence for iron-mediated anaerobic oxidation of methane. *Limnol Oceanogr* **56**: 1536–1544.

Slobodkina, G. B., Reysenbach, A.-L., Panteleeva, A. N., Kostrikina, N. A., Wagner, I. D., Bonch-Osmolovskaya, E. A., and Slobodkin, A. I. (2012) *Deferrisoma camini* gen. Nov., sp. nov., a moderately thermophilic, dissimilatory iron(III)-reducing bacterium from a deep-sea hydrothermal vent that forms a distinct phylogenetic branch in the Deltaproteobacteria. *Int J Syst Evol Microbiol* **62**: 2463–2468.

Stamatakis, A. (2006) RAxML-VI-HPC: maximum likelihood-based phylogenetic analyses with thousands of taxa and mixed models. *Bioinformatics* **22**: 2688–2690.

Stewart, F. J. (2011) Dissimilatory sulfur cycling in oxygen minimum zones: an emerging metagenomics perspective. *Biochem Soc Trans* **39**: 1859–1863.

Thamdrup, B., Finster, K., Hansen, J. W., and Bak, F. (1993) Bacterial disproportionation of elemental sulfur coupled to chemical reduction of iron and manganese. *Appl Environ Microb* **59**: 101–108.

Thamdrup, B., Fossing, H., and Jørgensen, B. B. (1994) Manganese, iron, and sulfur cycling in a coastal marine sediment, Aarhus Bay, Denmark. *Geochim Cosmochim Acta* **58**: 5115–5129.

Thauer, R. K., Kaster, A.-K., Seedorf, H., Buckel, W., and Hedderich, R. (2008) Methanogenic archaea: ecologically relevant differences in energy conservation. *Nat Rev Microbiol* **6**: 579–591.

Viollier, E., Inglett, P. W., Hunter, K., Roychoudhury, A. N., and Van Cappellen, P. (2000) The ferrozine method revisited: Fe(II)/Fe(III) determination in natural waters. *Appl Geochem* **15**: 785–790.

Vuillemin, A., Friese, A., Alawi, M., Henny, C., Nomosatryo, S., Wagner, D., *et al*. (2016) Geomicrobiological features of ferruginous sediments from Lake Towuti, Indonesia. *Front Microbiol* **7**: 1007.

Vuillemin, A., Horn, F., Alawi, M., Henny, C., Wagner, D., Crowe, S., and Kallmeyer, J. (2017) Preservation and significance of extracellular DNA in ferruginous sediments from Lake Towuti, Indonesia. *Front Microbiol* **8**: 1440.

Wang, G., Spivack, A. J., Rutherford, S., Manor, U., and D'Hondt, S. (2008) Quantification of co-occurring reaction rates in deep subseafloor sediments. *Geochim Cosmochim Acta* **72**: 3479–3488.

Zavarzina, D. G., Sokolova, T. G., Tourova, T. P., Chernyh, N. A., Kostrikina, N. A., and Bonch-Osmolovskaya, E. A. (2007) *Thermincola ferriacetica* sp. nov., a new anaerobic, thermophilic, facultatively chemolithoautotrophic bacterium capable of dissimilatory Fe(III) reduction. *Extremophiles* **11**: 1–7.

Zegeye, A., Bonneville, S., Benning, L. G., Sturm, A., Fowle, D. A., Jones, C. A., *et al*. (2012) Green rust formation controls nutrient availability in a ferruginous water column. *Geology* **40**: 599–602.

Zhang, J., Kobert, K., Flouri, T., and Stamatakis, A. (2014) PEAR: a fast and accurate Illumina paired-end reAd mergeR. *Bioinformatics* **30**: 614–620.

Zopfi, J., Ferdelman, T. G., and Fossing, H. (2004) Distribution of sulfur intermediates - sulfite, tetrathionate, thiosulfate, and elemental sulfur – in marine sediments. *GSA Special Papers* **379**: 97–116.

Supporting Information

Additional Supporting Information may be found in the online version of this article at the publisher's web-site:

Fig. S1. Multiple sediment downcores obtained for the shallow and deep site. From left to right: (A) Calcium, magnesium, ammonium, dissolved iron, chloride and sulfate concentrations [μM] measured in the pore water; potential sulfate reduction rates [nmol × cm^{-3} day^{-1}]. (B) Total organic carbon, total carbon [weight %] and molar C_{org} /N ratio measured in bulk sediments; cell counts in log scale [log10 cells × cm^{-3}]; concentrations of extracellular DNA (grey dots) and total DNA (black squares) [μg × g^{-1} wet sed], with distance between the two curves corresponding to intracellular DNA concentrations; Shannon index established from bacterial and archaeal DGGE gel features, with eDNA (grey dots) and iDNA (black squares) displayed separately (from Vuillemin *et al.,*).

Fig. S2. Relative abundances, phylogenetic tree and functional gene affiliation for Bathyarchaeota sequences. (A) Bar charts displaying the relative abundances of sequences affiliated with Bathyarchaeota. (B) Maximum Likelihood phylogenetic tree based on partial 16S rRNA gene sequences established for Bathyarchaeota representative OTUs. (C) Taxonomic affiliation for the *mcrA-G* and *fhs* gene presently including 12 and 4 sequences identified as Bathyarchaeota, respectively.

Fig. S3. Canonical correspondence analysis based on 12 environmental parameters with representative operational taxonomic units. The distribution of samples for the shallow and deep site reflects a depth trend as shown by all significant variables of the triplot (insert down left). Taxa can be successively traced from left to right to infer species related to iron, sulfur and hydrogen cycling with sediment depth.

Fig. S4. KEGG pathways involved in methane production. Metagenomes from both sites were screened to identify carbon substrates used in methane production. Subunits of the *mtr*, *cdhA*, *CODH*, *fdh*, *mta*, *mtb*, and *mtsA* gene were exported from the JGI platform and assigned using BLASTp. Results demonstrate that microbial communities have the metabolic potential to produce methane from H_2/CO_2, formate, methanol, methylamines and methylated thiols. Additionally we assigned taxonomically sequences from the *mcrA*, *MtrA* and *hdrA* gene to provide an overview of the microbial assemblage involved in ferredoxin functions and methane production. The corresponding bar charts are displayed in Supplementary Fig. S6. The present KEGG pathway diagram is modified after the IMG/MER workspace of the JGI website.

Fig. S5. KEGG pathways involved in sulfur metabolism. Metagenomes from both sites were screened to identify genes involved in sulfur redox processes. Subunits of the *dsr*, *apr*, *phs*/*psr*, *asr*, *hydB*, *sox* and *SUOX* were exported from the JGI platform and assigned using BLASTp. Results demonstrate that microbial communities have the metabolic potential to cycle sulfur compounds anaerobically. The

corresponding bar charts are displayed in Supplementary Fig. S6. The present KEGG pathway diagram is modified after the IMG/MER workspace of the JGI website.

Fig. S6. Affliliations of functional genes. (Left) Taxonomic assignment for functional genes corresponding to formate dehydrogenase (*fdh*), methanol coenzyme M methyltransferase (*MtaB*), methyaminespecific coenzyme M methyltransferase (*MtbA*), methylthiol: coenzyme M methyltransferase (*mtsA*), carbonmonoxide dehydrogenase (*CODH*), acetyl-CoA decarbonylase (*cdhA*), methyl-coenzyme M reductase (*mcrA*), tetrahydromethanopterin S-methyltransferase (*mtrA*), and heterodisulfide reductase (*hdrA*). Results provide evidence for the metabolic potential of diverse archaeal taxa to produce methane from different carbon substrate, namely formate, methanol, methylamines, methylated thiols and H_2/CO_2. (Right) Taxonomic assignment for functional genes corresponding to dissimilatory sulfite reductase (*dsr*), adenylylsulfate reductase (*apr*), anaerobic sulfite reductase (*asr*), thiosulfate/polysulfide reductase (*phs*/*psr*), sulfhydrogenase or sulfur reductase (*hydB*), sulfur-oxidizing protein (*sox* subunits B, C, D, X, Y) and sulfite oxidase (*SUOX*). Results show that the microbial consortium composed of Deltaproteobacteria, Firmicutes, Nitrospirae and Chloroflexi to reduce sulfate, sulfite, thiosulfate, sulfur and polysulfide anaerobically and, theoretically, to reverse oxidize these compounds anaerobically. Detection of functional genes related to aerobic oxidation of sulfur compounds was low and mainly revealed taxa preserved from the water column (e.g. Chlorobi, Cyanobacteria, Betaproteobacteria).

Table S1. Table summarizing the number of representative OTUs per phyla and relative abundances for each metabolic category. Relative abundances are listed according to sample depth for the shallow (0.5, 7.5, 15.0, 27.5 cmblf) and deep (1.5, 7.5, 15.0, 32.5 cmblf) sites. Unresolved OTUs correspond to the different candidate divisions plotted in the phylogenetic trees (Figs A -D).

Table S2. Table summarizing taxonomic assignments of functional genes: From left to right: *dsrAB*, *aprA*, *mcrA* and *fhs* genes.